Supplementary Information for

Template-free synthesis of honeycomb-structured Ta_3N_5 foam nanoplates with expanded light absorption, abundant active sites and fast charges transport for visible-light-driven H_2 evolution

Jiudi Zhang[a‡], Ruyu Zhang[b,c‡], Xiaowei Jia[a,], Jinming Li[a], Mingliang Sun[b], Shikang Zhang[a], Zhenfu Guo[a], Xiaoyan Jiao[a], Xianchun Liu[b], Zhanshuang Jin[a], Junjie Li[a,*], Yan Xing[b,*]*

[a]College of Science, Hebei North University, Zhangjiakou 075000, P. R. China

[b]College of Chemistry, Northeast Normal University, Changchun 130024, P. R. China

[c]School of Light Industry and Chemical Engineering, Dalian Polytechnic University, Dalian 116034, P. R. China

*Corresponding Authors

E-mail address: jiaxw813@nenu.edu.cn (X. Jia); Ljj8966@163.com (J. Li); xingy202@nenu.edu.cn (Y. Xing)

‡These authors contributed equally to this work.

1. Experimental section

1.1 Characterization techniques

The crystal phases of the as-obtained samples were characterized by powder X-ray diffraction (XRD) on a Siemens D5005 diffractometer with Cu Kα radiation (λ = 1.5418 Å) operated at 40 kV and 40 mA. The scans were performed in the 2θ range of 10-80° with a step size of 0.02° and a counting time of 1 s per step. Scanning electron microscopy (SEM, Hitachi SU8010), transmission electron microscopic (TEM, JEM-2100F), high-resolution transmission electron microscopy (HRTEM, JEM-2100F) and energy-dispersive X-ray spectroscopy (EDX, JEM-2100F) were employed to study the morphology, nanoparticle sizes, lattice parameters and element mapping of the photocatalysts. For SEM imaging, the samples were dispersed in ethanol via ultrasonication for 10 min, dropped onto a silicon wafer, and dried under ambient conditions. For TEM analysis, the samples were similarly dispersed in ethanol, dropped onto a carbon-coated copper grid, and dried at room temperature. The X-ray photoelectron spectroscopy (XPS, Thermo ESCALAB 250 instrument) with a monochromatic source (Al Kα $h\nu$ = 1486.6 eV) was carried out to identify the chemical compositions and chemical valence of the samples. The XPS spectra were calibrated using the C 1s peak (284.8 eV) as an internal reference. Deconvolution analysis was performed using XPSPEAK software (version 4.1) with a Shirley background and mixed Gaussian-Lorentzian (70:30) line shapes. The full width at half maximum (FWHM) was constrained to 1.0-1.8 eV for all peaks. The ultraviolet-visible diffuse reflectance spectroscopy (UV-vis DRS, Agilent Cary 7000) with $BaSO_4$ as a reference

was used to identify the optical properties. The specific surface area and pore size distribution were determined via nitrogen adsorption-desorption isotherms at 77 K using a Micromeritics Tristar 3000 analyzer. Prior to analysis, the sample was degassed under high vacuum at 150°C for 6 hours to eliminate adsorbed moisture and contaminants. The Brunauer-Emmett-Teller (BET) surface area was calculated from the adsorption branch in the relative pressure (P/P_0) range of 0.05-0.30. The pore size distribution was derived from the desorption branch using the Barrett-Joyner-Halenda (BJH) method, and the total pore volume was evaluated at $P/P_0 = 0.99$. The photoelectrochemical/electrochemical measurements were carried out using the CHI 660E electrochemical workstation (Chenhua, Shanghai). During this test, a standard three-electrode system was adopted, in which Pt sheet, saturated calomel electrode (SCE), photocatalysts/ITO and 0.5 M Na_2SO_4 solution were acted as the counter electrode, reference electrode, working electrode and electrolyte, respectively.

2. Results

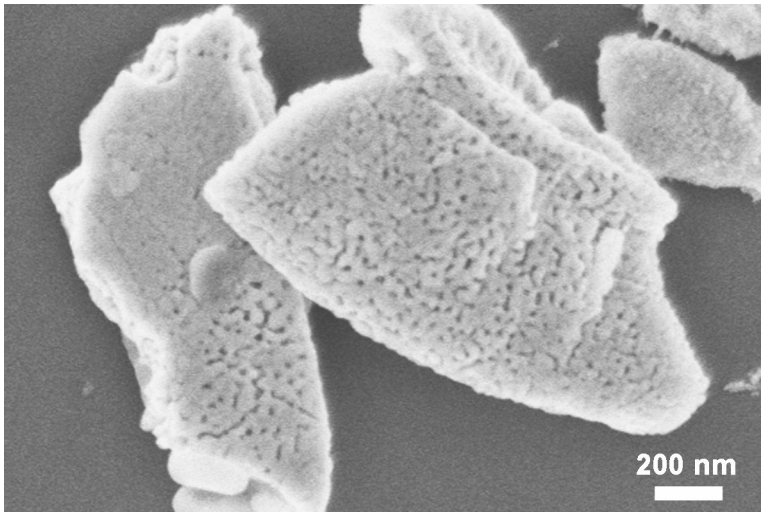

Fig. S1. SEM image of the honeycomb-structured TaO_x nanoplate.

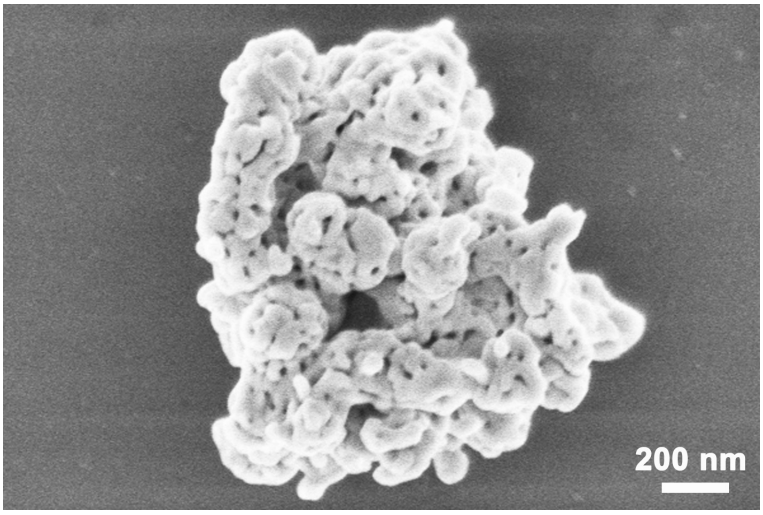

Fig. S2. SEM image of the bulk Ta_3N_5 nanoparticles.

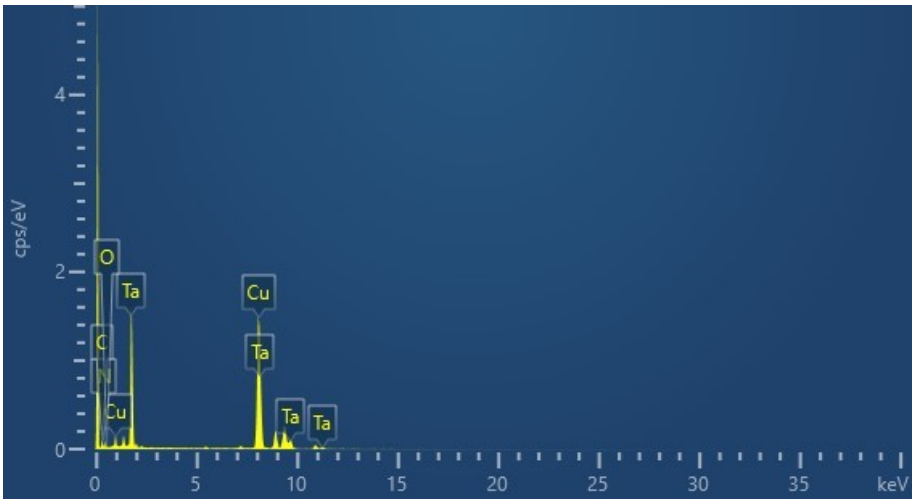

Fig. S3. EDX spectrum of the honeycomb-structured Ta_3N_5 nanoplates.

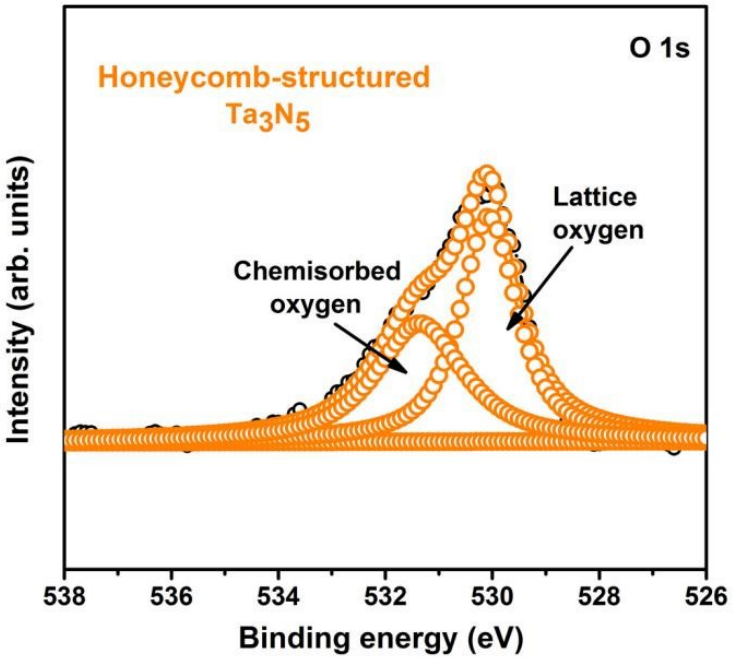

Fig. S4. O 1s XPS spectra of the honeycomb-structured Ta_3N_5 foam nanoplates.

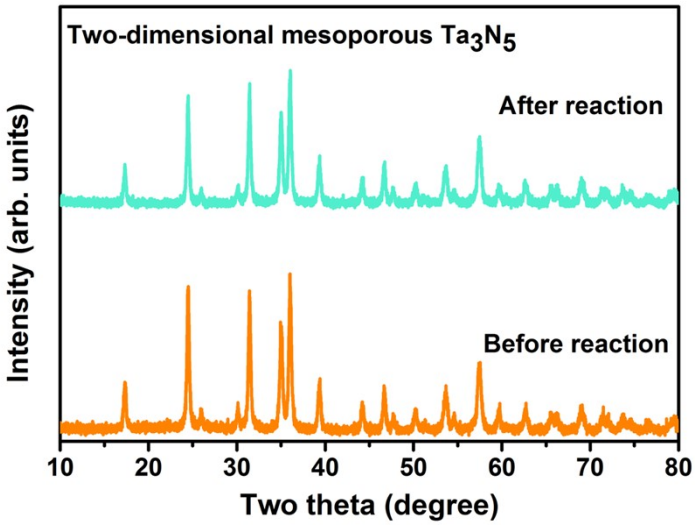

Fig. S5. XRD pattern of honeycomb-structured Ta_3N_5 nanoplate after the photocatalytic H_2 evolution reaction.

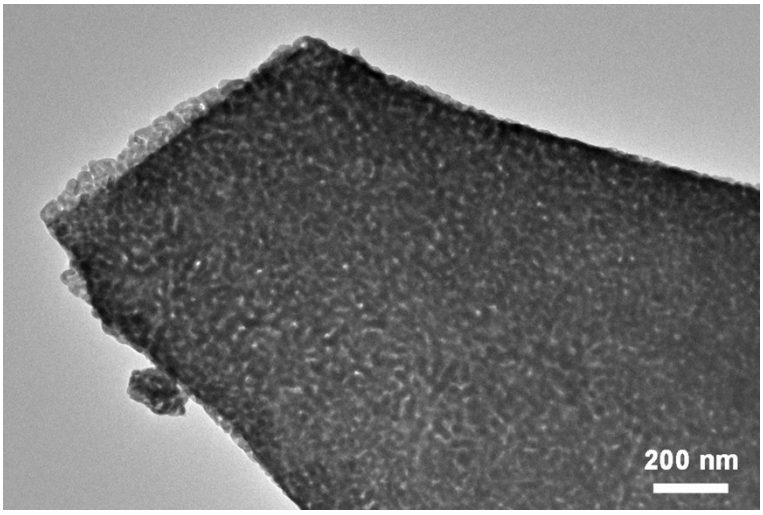

Fig. S6. TEM image of honeycomb-structured Ta_3N_5 nanoplate after the photocatalytic H_2 evolution reaction.

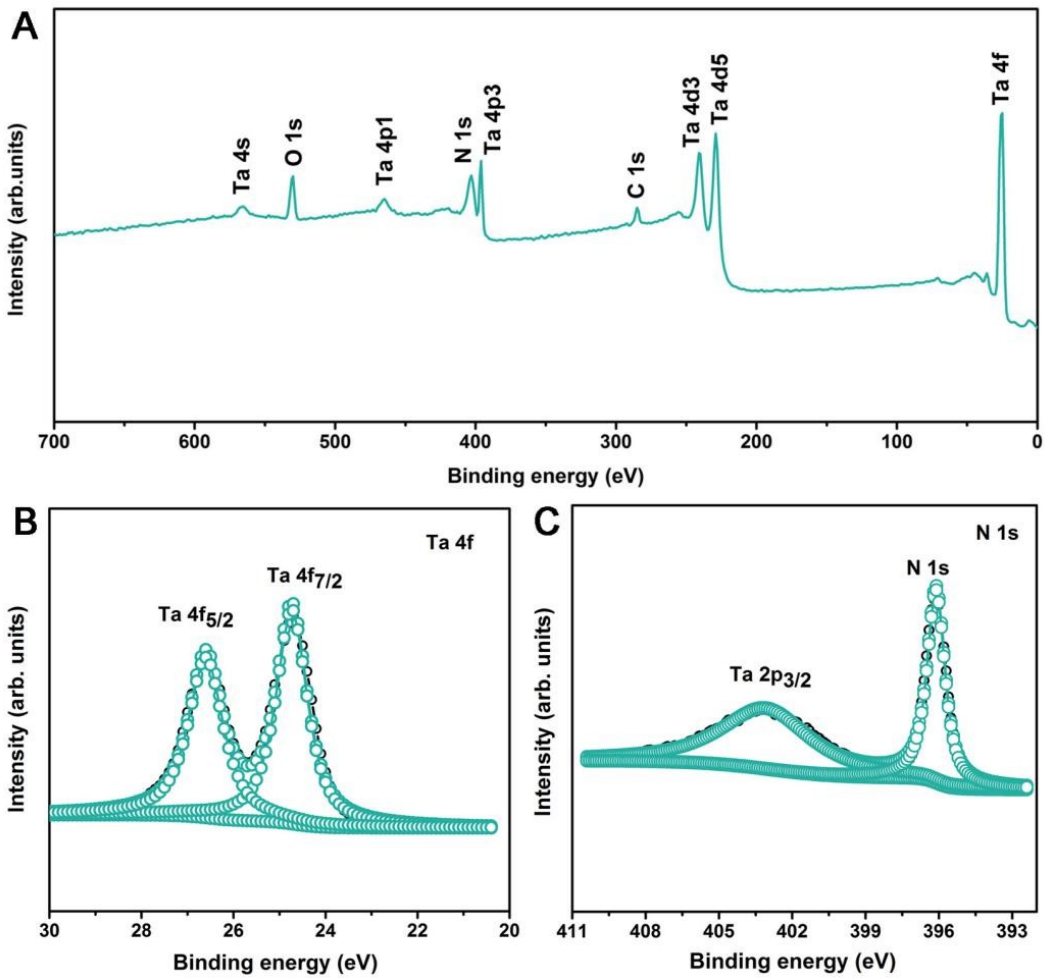

Fig. S7. XPS spectra of the honeycomb-structured Ta_3N_5 foam nanoplates after the photocatalytic H_2 evolution. (A) XPS survey spectrum, high resolution spectra for (B) Ta 4f and (C) N 1s.

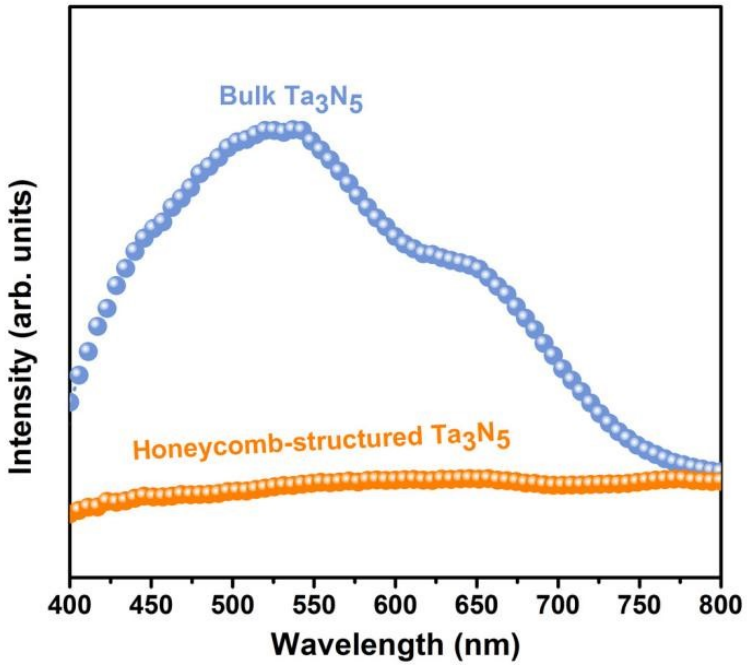

Fig. S8. Steady-state PL spectra of bulk Ta_3N_5 and honeycomb-structured Ta_3N_5.

Table S1. The comparison of photocatalytic hydrogen production performance for honeycomb-structured Ta_3N_5 and other previously reported morphologies of Ta_3N_5 photocatalysts in recent years.

Photocatalyst	***Weight (mg)***	***Light source (nm)***	***H_2 (μmol h^{-1} g^{-1})***	***Ehancement fators vs. Ta_3N_5***	***Ref.***
Ta_3N_5 nanoplates	20	$\lambda > 400$	26.5	17.7	S1
Ta_3N_5 octahedra	20	$\lambda > 400$	17.0	11.3	S1
Ta_3N_5 nanomeshes	20	AM 1.5G	575.0	10.0	S2
Ta_3N_5 nanosheets	50	AM 1.5G	65.8	5.3	S3
Ta_3N_5 nanosheet	1	$\lambda > 550$	2.1	N/A	S4
Ta_3N_5 single-crystal	100	$\lambda > 420$	33.0	5.0	S5
mesoporous Ta_3N_5	30	$\lambda > 420$	34.6	3.9	S6
Honeycomb-structured Ta_3N_5	**50**	**$\lambda > 420$**	**59.16**	**22.7**	**Our work**

Reference

[S1] J. Fu and S. E. Skrabalak, *J. Mater. Chem. A*, 2016, **4**, 8451-8457.

[S2] M. Xiao, B. Luo, M. Lyu, S. Wang and L. Wang, *Adv. Energy Mater.*, 2018, **8**, 1701605.

[S3] Q. Guo, J. Zhao, Y. Yang, J. Huang, Y. Tang, X. Zhang, Z. Li, X. Yu, J. Shen and J. Zhao, *J. Colloid Interface Sci.*, 2020, **560**, 359-368.

[S4] C. Hsu, K. Awaya, M. Tsushida, T. Sato, M. Koinuma and S. Ida, *ChemistrySelect*, 2020, **5**, 13761-13765.

[S5] J. Cui, T. Liu, B. Dong, Y. Qi, H. Yuan, J. Gao, D. Yang and F. Zhang, *Sol. RRL*, 2021, **5**, 2000574.

[S6] Q. Yang, Y. Li, Z. Xia, W. Chang and Y. Xing, *Ceram. Int.*, 2022, **48**, 22297-22304.